

## Algorithms for intelligent prediction of landslide displacements<sup>\*</sup>

Zhong-qiang LIU<sup>1</sup>, Dong GUO<sup>2</sup>, Suzanne LACASSE<sup>†‡1</sup>, Jin-hui LI<sup>†‡2</sup>, Bei-bei YANG<sup>3</sup>, Jung-chan CHOI<sup>1</sup>

<sup>1</sup>Norwegian Geotechnical Institute (NGI), Oslo 0855, Norway

<sup>2</sup>Department of Civil and Environmental Engineering, Harbin Institute of Technology (Shenzhen), Shenzhen 518055, China

<sup>3</sup>School of Engineering, Yantai University, Yantai 264005, China

<sup>†</sup>E-mail: suzanne.lacasse@ngi.no; jinhui.li@hit.edu.cn

Received Jan. 11, 2020; Revision accepted May 15, 2020; Crosschecked May 23, 2020

**Abstract:** Landslides represent major threats to life and property in many areas of the world, such as the landslides in the Three Gorges Dam area in mainland China. To better prepare for landslides in this area, we explored how several machine learning algorithms (long short term memory (LSTM), random forest (RF), and gated recurrent unit (GRU)) might predict ground displacements under three types of landslides, each with distinct step-wise displacement characteristics. Landslide displacements are described with trend and periodic analyses and the predictions with each algorithm, validated with observations from the Three Gorges Dam reservoir over a one-year period. Results demonstrated that deep machine learning algorithms can be valuable tools for predicting landslide displacements, with the LSTM and GRU algorithms providing the most encouraging results. We recommend using these algorithms to predict landslide displacement of step-wise type landslides in the Three Gorges Dam area. Predictive models with similar reliability should gradually become a component when implementing early warning systems to reduce landslide risk.

**Key words:** Landslide; Displacement; Machine learning; Three Gorges Dam reservoir  
<https://doi.org/10.1631/jzus.A2000005>

**CLC number:** P642

### 1 Introduction

Landslides are one of the most damaging disasters in many areas of the world, resulting in significant losses of life, property, and environmental resources. The China Institute of Geo-environment Monitoring reported that 9710 geology-related hazards occurred in China in 2016, 7403 of which were landslides (CIGM, 2017). The 2017 Maoxian landslide damaged 62 houses and buried over 100 people (Intrieri et al., 2018).

The Three Gorges Dam reservoir (China) is a landslide-prone area. The construction of the Three Gorges Dam significantly increased hazard risks to

people, property, and the environment from landslides in and around the dam and reservoir (Bai et al., 2010). These risks could be reduced by a reliable early warning system if systems could reliably predict landslide displacements with reasonable accuracy and if the system could set reliable displacement thresholds for early warning. Zhou et al. (2016) reported that in the area of the 1985 Xintan landslide (26 km upstream from the Three Gorges Dam), the economic losses and the number of fatalities were significantly reduced by an warning system that provided a reasonably reliable prediction of the landslide displacements.

Forecasting of landslide deformation can be done through either physical or data-based models (Ran et al., 2012; Huang et al., 2016). The displacement process of landslides is complex, making it challenging to build physical models that are sufficiently representative. On the other hand, three categories of data-based forecasting models (deterministic, statistical, and computational intelligence models

<sup>‡</sup> Corresponding author

<sup>\*</sup> Project supported by the Research Council of Norway and the National Natural Science Foundation of China (No. 51979067)

 ORCID: Zhong-qiang LIU, <https://orcid.org/0000-0002-1693-5746>

© Zhejiang University and Springer-Verlag GmbH Germany, part of Springer Nature 2020

(Ma et al., 2017)), which involve physical mechanisms and general creep theory, can provide explanations for landslide processes. These forecasting models, however, apply only to specific cases, rarely consider 3D effects, involve uncertainties that are difficult to quantify, and incorporate external activities (rainfall, reservoir rise or drawdown) that are difficult to model. Statistical models also have limitations as they are only valid for landslides with comparable deformation characteristics. These sorts of models usually result in widely scattered predictions of landslide deformations such as the runout distance of clays (McDougall, 2017).

These shortcomings have been addressed in recent years through advances in artificial intelligence, especially machine learning algorithms, that have greatly improved modelling and forecasting of landslide deformation (Liu et al., 2014; Ma et al., 2018; Yang et al., 2018). This paper compares three machine learning algorithms (long short term memory (LSTM), random forest (RF), and gated recurrent unit (GRU)) to predict landslide hazards from measured behavior and measured external actions. The modeling, if successful, could help reduce the future risk associated with landslide hazards. This paper aims at demonstrating the maturity of machine learning algorithms and their ability to predict landslide displacement. Three landslides are used to construct and validate the machine learning models. The paper briefly describes the landslides and the machine learning algorithms used and then compares the results of the analyses.

## 2 Three step-wise landslides in Three Gorges Dam reservoir

### 2.1 Three Gorges Dam reservoir area

In the Three Gorges Dam reservoir area, movements in active landslides have intensified and past landslides have been reactivated by intense rainfall and/or the raising and lowering of the dam water reservoir. Corominas and Moya (2005), among others, showed that meteorological data indicate that increased movements are often closely related to seasonal rainfall. In the proximity of dams, fluctuations in the reservoir water level can also significantly influence the behavior of the slopes within the reservoir (Yang et al., 2017). When the Three Gorges Dam reservoir was impounded in 2003, the 14 million m<sup>3</sup> Qianjiangping landslide was reactivated when the reservoir water level reached 135 m, leading to many casualties and extensive damage. When the reservoir water level was raised to 172 m in 2008, 60 landslides were triggered or reactivated, again causing widespread damage (Du et al., 2013).

Fig. 1 shows the Yangtze River and its tributaries, the location of the Three Gorges Dam, and the locations of the three landslides that are the focus of this research. In the Three Gorges Dam reservoir area, many of the landslides show a step-wise displacement curve. In this work, the step-wise Baishuihe, Baijiabao, and Bazimen landslides (Fig. 1), will be used to develop the machine learning models and to predict future displacements.

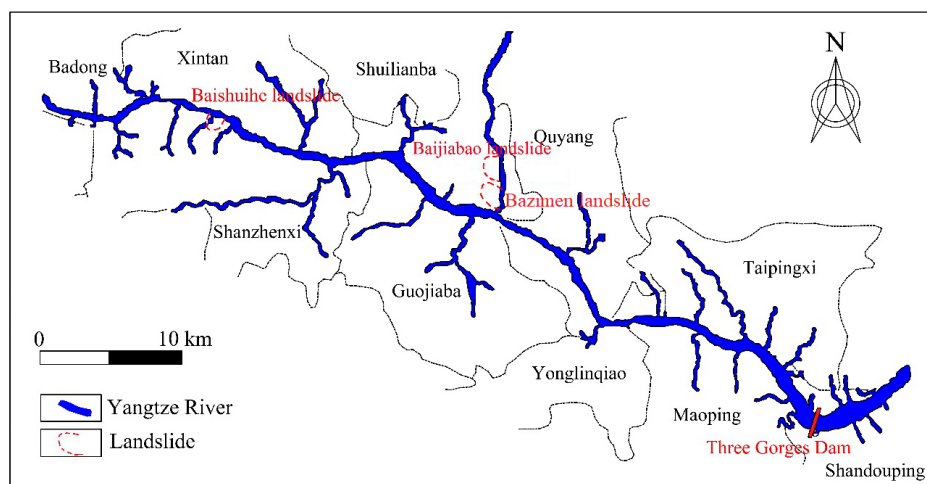


**Fig. 1** Yangtze River, Three Gorges Dam reservoir area, and three landslides studied. Reprinted from (Yang et al., 2019b), copyrights 2019, with permission from Springer Science+Business Media

## 2.2 Baishuihe landslide

The Baishuihe landslide is located about 56 km from the Three Gorges Dam. The 2003 landslide measured 700 m from east to west, 780 m from north to south, and extended over  $4.2 \times 10^5 \text{ m}^2$ . The moving masses had an average thickness of 30 m and an estimated volume of  $1.26 \times 10^7 \text{ m}^3$ . Baishuihe landslide has been reactivated frequently including periods of severe deformation and over time has caused extensive damage including the destruction of 21 residential houses in 2004, and the evolution of transversal cracks on the landslide surface (August 2005 to August 2006), along with sizeable road debris pileup (Yang et al., 2019b).

From 2003 to 2013, the Baishuihe landslide movements developed features of a retrogressive landslide with deformations at the bottom of the slope that gradually progressed upwards (Du et al., 2013; Miao et al., 2018). Due to the large displacements and associated potential risks from these movements, 11 global positioning system (GPS) stations were installed. Fig. 2 shows related data from 2003–2013, including the GPS recorded displacements, reservoir water levels, and rainfall at Location ZG118 as this area had the largest quantity of data and largest observed displacements. Data indicate three periods of fluctuation in the water levels in the Three Gorges reservoir:

(1) August 2003 to August 2006: water level ran between 135 m and 139 m. During that time, only a small portion of the slope was under water. The effect of the change in reservoir water level was small. The accumulated displacement at Location ZG118 was step-wise from May to September, in tandem with the start of the reservoir level change and annual intense rainfall season.

(2) September 2006 to September 2008: the reservoir water level varied between 145 m and 155 m, causing a large volume of the slope to be submerged. When the reservoir level rose, the displacement increased slowly. When the reservoir water level fell from 155 m to 145 m concurrent with a rainfall of 685 mm (July 2007), the largest deformation to date occurred with a displacement of 334 mm in one month.

(3) October 2008 to December 2013: the water level in the reservoir varied between 145 m and 175 m. When the reservoir water level fell for the first time from 175 m to 145 m, this time under a rainfall of 626.4 mm, the maximum monthly displacement was only 98.9 mm, which was much less than the maximum monthly displacement of 334 mm in the second period. The annual displacement maintained a step-wise behavior during each flood season, although the magnitude of each step decreased with time.

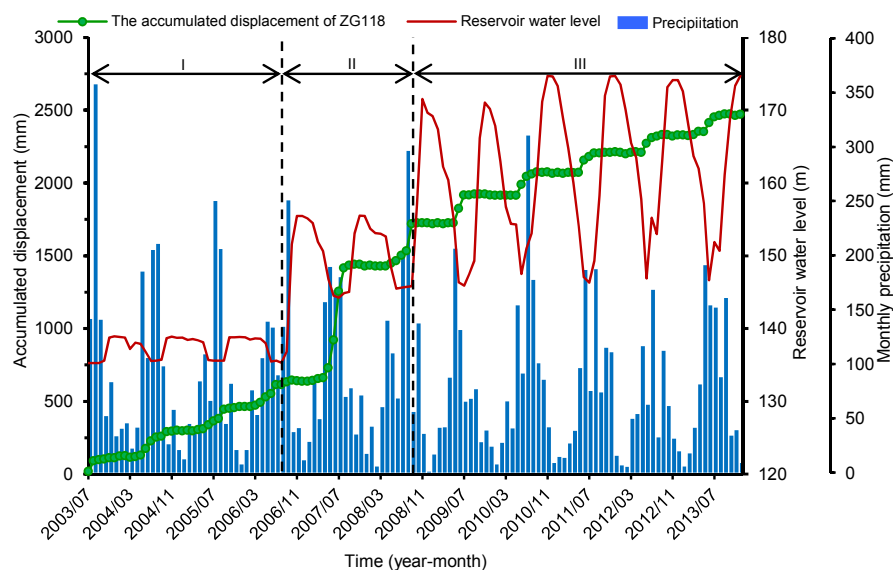


**Fig. 2** Recorded rainfall, reservoir water level, and displacement in Baishuihe landslide. Reprinted from (Yang et al., 2019b), copyrights 2019, with permission from Springer Science+Business Media

### 2.3 Bazimen landslide

The Bazimen landslide close to the town of Zigui, was fan-shaped and extended over a  $1.35 \times 10^5 \text{ m}^2$  area. The landslide had a maximum length of 380 m, width of 100 to 350 m, and a moving mass volume estimated as  $2 \times 10^6 \text{ m}^3$  (Yang et al., 2019a). There were two main sliding surfaces, one at about 10 m depth, the other at about 30 m depth. After dam impoundment, the Bazimen landslide started to move again and two sizable cracks appeared on each side of the road within the area in August 2003. As the rainfall season unfolded in 2004 (May to August), several cracks were observed within the landslide area as the reservoir water level dropped from 139 m to 135 m. GPS monitoring points were installed on the Bazimen landslide at elevations of 165 m, 191 m, and 215 m (Du et al., 2013). The observed displacements in the upper region (Location ZG111) were larger than those in other parts within the landslide.

The Bazimen landslide behaved as a “progressive” landslide, where the movements started from the upper part and gradually developed downwards (Du et al., 2013; Zhou et al., 2016). We selected Location ZG111 for machine learning model of displacements because this area had the longest series of available data and the largest deformations. Fig. 3 shows the measured displacement, reservoir water

levels, and rainfall at Location ZG111 from 2003 to 2012. Significantly larger displacements were observed at the Baishuihe landslide during and after the first large drawdown in 2009. The step-wise displacements, however, did not decrease with time in the subsequent years and intense rainfall (2008 and 2010) did not result in the largest displacements.

### 2.4 Baijiabao landslide

The Baijiabao landslide, also close to the town of Zigui, is located next to the Bazimen landslide. The front part of the area was submerged in the dam reservoir. The toe of the landslide was at an elevation of 135 m, and the upper edge was at an elevation of 265 m. The landslide was 550 m long from east to west and 400 m wide from north to south. Landslide debris had an average thickness of 45 m and extended over a volume of about  $9.9 \times 10^6 \text{ m}^3$  (Cao et al., 2016). With the 2003 impoundment of the dam reservoir, many cracks appeared on the landslide. In late July 2003, after a long and intense rainfall, different levels of deformation developed on the ground surface, in houses on the upper edge of the landslide, and in the road in the middle of the landslide.

In late 2006, four GPS stations were installed on the Baijiabao landslide to monitor potential risks developing there. Based on analyses of the movements of the Baijiabao landslide, Cao et al. (2016)

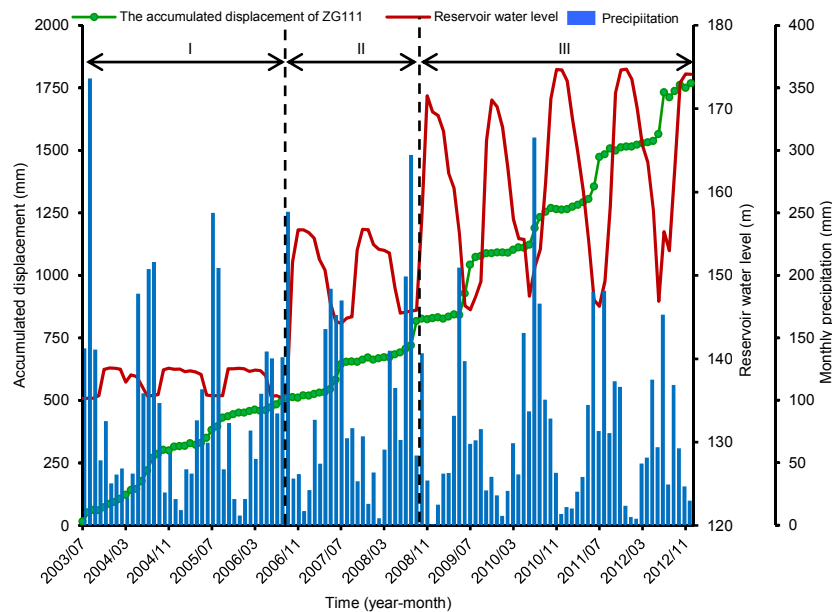


**Fig. 3** Recorded rainfall, reservoir water level, and displacement in Bazimen landslide. Reprinted from (Yang et al., 2019b), copyrights 2019, with permission from Springer Science+Business Media

suggested that the Baijiabao landslide deformed as an entity (Yang et al., 2019a). The monitored displacement at Location ZG324 at the center of the landslide was used to establish the machine learning models. Fig. 4 shows the accumulated displacements at Location ZG324 versus time as well as the measured rainfall and reservoir water level. Each year, displacements increased from May to September, during periods of reservoir water drawdown and seasons of heavier precipitation. The reservoir level was raised each October and held constant (about 175 m) until the following April. During these periods, precipitation was gentle and the landslide displacement was minimal. The combined action of seasonal rainfall and reservoir drawdown caused step-wise increases in displacement.

### 3 Approach to model displacements in Three Gorges Dam reservoir

#### 3.1 Time series decomposition

The displacement ( $D$ ) was decomposed into three components: a trend, a periodic, and a stochastic component, i.e.

$$D = \phi + P + S. \quad (1)$$

The long-term displacement, controlled by “internal” geological conditions such as lithology, geological structure, and progressive weathering, was the trend component ( $\phi$ ). The short-term displacement was influenced by two “external” factors of rainfall and dam reservoir water levels, represented as the periodic component ( $P$ ). The stochastic term ( $S$ ) is the displacement response caused by a sudden change such as a raise or drop of the reservoir level. Du et al. (2013) pointed out that in the Three Gorges Dam reservoir, the reservoir level changes regularly on an annual cycle. The total displacement measured by the monitoring system, therefore, can also be divided into trend and periodic terms and each can be predicted separately by different methodologies.

#### 3.2 Trend component

The trend term in the displacement vs time curve was extracted by the moving average method, and the trend term at time  $t$ ,  $\phi(t)$ , was calculated as follows:

$$\phi(t) = \frac{D_t + D_{t-1} + \dots + D_{t-k+1}}{k}, \quad (2)$$

$$t = k, k+1, \dots, n,$$

where  $D_t$  is the total displacement at time  $t$ ,  $n$  is the

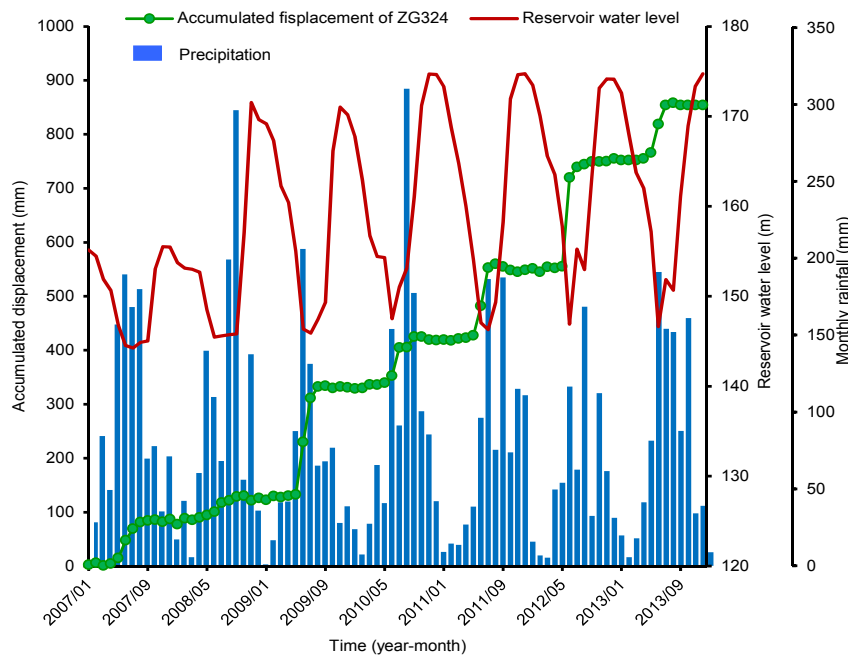


Fig. 4 Recorded rainfall, reservoir water level, and displacement in Baijiabao landslide

number of measured accumulated displacement points, and  $k$  is the moving average cycle.

The trend displacement was predicted with a cubic polynomial function (Yang et al., 2019b) of the form in Eq. (3):

$$\phi(t)=at^3+bt^2+ct+d, \quad (3)$$

where  $a$ ,  $b$ ,  $c$ , and  $d$  are coefficients (where  $a$  cannot be zero). The trend displacement polynomial function was fitted by the MATLAB R2015b software.

### 3.3 Periodic component

The periodic term in the displacement vs time curve was predicted by multivariate machine learning algorithms to model the relationship among landslide displacement and rainfall and dam reservoir water level. To verify the performance of the models, the latter part of the observed displacements was not included in the model development and was used to compare with the predictions made by the machine learning models.

For the machine learning models, key influence factors were selected as the input sequences and designated periodic displacement as output sequences (Section 4). Rainfall and reservoir water level were input sequences because they are external influence factors on the displacement. Selby (1988) suggested that the state of evolution of a landslide was also an important factor affecting the way the movement responded to the external factors. Following Cao et al. (2016) and Zhou et al. (2018a, 2018b), rainfall, dam reservoir water level, and the state of the landslide were selected as the key factors influencing the periodic displacement in the machine learning models.

## 4 Machine learning algorithms implemented

Qin et al. (2002) have shown that the movement of an active landslide is a nonlinear dynamic process. The deformation conditions and triggers at a given time affect the deformation in the following time interval (Xu and Niu, 2018). Most of the existing prediction models are static and ignore the dynamic characteristics of landslides. Recurrent neural networks (RNNs) (e.g. LSTM and GRU) are dynamic

models that can remember information from earlier time interval(s) and apply the knowledge learned from the earlier step(s) to the next step (Han et al., 2004; Chen and Chou, 2012).

Table 1 lists the statistical and machine learning models used to analyze the landslides in the Three Gorges Dam reservoir. The purpose of the study is to compare the reliability of these algorithms, to determine if one or more are robust enough to accurately predict landslide displacements, and to decide if any might be useful to inform decision-making in early warning systems in the Three Gorges Dam area. The modelling was done separately for each of these landslides and data were not combined because each landslide had different monitoring locations and was influenced by different factors.

**Table 1 Machine learning algorithms for analysis of Three Gorges Dam reservoir landslides**

Landslide	Statistical and machine learning models	
	Trend	Periodic displacement
Baishuihe	3rd degree polynomial	LSTM RF GRU
Bazimen	3rd degree polynomial	LSTM RF GRU
Baijiabao	3rd degree polynomial	LSTM RF GRU

In this paper, three different prediction models was developed for each of the three landslides. This section only briefly describes the machine learning algorithms used, as more details are available in (Cho et al., 2014; Yang et al., 2019b; Liu et al., 2020).

### 4.1 Long short term memory neural network model

LSTM neural network belongs to the dynamic RNNs category. These networks can model temporal sequences and time dependencies more reliably than conventional RNNs, which in general cannot handle long sequences (Vincent et al., 2010; Li et al., 2020). The LSTM neural network includes an input layer, one or several hidden layer(s), and an output layer. Fig. 5 illustrates the structure of an LSTM neural network at a given time-step. The basic unit of the hidden layer is a memory block and the units in the hidden layer are related to other units from one step to

another. The memory block consists of an input gate, a forget gate, an output gate, and a memory cell. The three gates are responsible for regulating the flow of information in and out of the memory cell. The input gate controls the flow of input activations into the memory cell. The forget gate controls whether the information from the previous step is remembered or forgotten. The output gate is responsible for transferring useful information to the next memory block. Yang et al. (2019b) described the LSTM neural network algorithm used in more detail. The LSTM model for landslide displacement modelling is interesting because it reflects the dynamic evolution of deformations by relating observations from one time-step to the next.

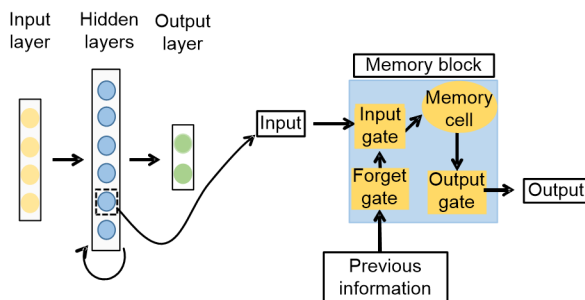


**Fig. 5** Structure of an LSTM neural network at a given time-step

## 4.2 Random forest algorithm

The RF algorithm is an “ensemble” machine learning method for classification and regression and consists of the definition of multiple decision trees first developed by Breiman (2001). The RF algorithm generates uncorrelated decision trees that operate together. The RF algorithm creates an ensemble of random decision trees and forms a forest to produce more accurate ensemble prediction. Each tree is grown based on a re-sampling (bootstrap aggregating) technique. The classification and regression procedure are established through a random group of variables selected at each tree node (Breiman, 2001). To ensure reliable predictions, at least two conditions should be verified: the selected variables should have some predictive power ability; the different decision tree models need to be uncorrelated (Liu et al., 2020). Detailed statistical explanation on RF algorithm is given in (Breiman, 2001).

## 4.3 Gated recurrent unit algorithm

The GRU algorithm belongs to the RNN category. Traditional RNN trains the neural network model by using gradient-based methods. Gradient-based methods learn neural network’s parameters by learning how small changes in the network’s parameters will affect network output. The network cannot effectively learn the network’s parameter when a change in the network’s parameter causes very small change in the network’s output. When training certain artificial neural networks using gradient-based methods, the vanishing gradient problem can occur and become gradually worse with increases in the number of layers in the architecture. In the vanishing gradient problem, the gradients of the network’s output relative to the network’s parameter in the early layers become extremely small: even a large change in the network’s parameter of the early layers does not have a big effect on the network’s output. Therefore, it is difficult to learn and tune the network’s parameter of earlier layers when the vanishing gradient problem appears. To solve the vanishing gradient problem of a standard RNN, GRU uses the so-called update gate and reset gate (Cho et al., 2014). The GRU algorithm has a simpler memory block structure than the LSTM, with a reset gate and an update gate only. Fig. 6 illustrates the structure of the GRU network. The reset gate decides how much information from the previous step is remembered and resets the information in the current time-step. The update gate helps the model determine how much information from previous steps and the current information needs to be transferred to the cell and ultimately sent to the output layer.

## 5 Analysis input and key factors for periodic displacement modelling

### 5.1 Input for periodic displacement model

Slopes at different stability states can respond differently under the impulse of identical external trigger factors. For a stable slope, even strong triggers may not cause excessive displacements. On the other hand, for a marginally stable or unstable slope, the slightest increase in an external “load” may cause

disequilibrium and large displacements (Crozier and Glade, 2005). As mentioned, rainfall (or precipitation) and dam reservoir water level were used as input sequences because they are believed to act as triggers for slope displacements. In the case of the three landslides modelled here, the displacement was measured by GPS once a month. In the machine learning models, the time interval between two different time frames changed with landslide deformation characteristics and actual demand. From April to September, the landslides deformed in distinct steps. The interval between two time frames was short, e.g. one month. In modelling, the interval can be shorter if more data are available during the same monitoring period. From October to April, the sliding became more uniform again. The interval between two time frames can be longer during this period. The displacements recorded over periods of one, two, and three months were selected as the most significant parameters to represent the current state of the slope (Cao et al., 2016; Zhou et al., 2016, 2018a). Table 2 lists the key input parameters selected for the analysis of the periodic displacements of the three landslides.

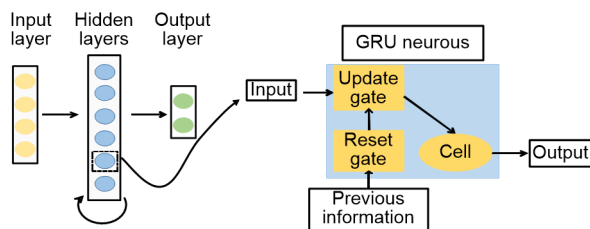


Fig. 6 Structure of a GRU neural network at a given time-step

## 5.2 Importance of key factors influencing periodic displacement

Several techniques can be used to quantify the predictive capacity of influence factors including the information gain ratio (Tien Bui et al., 2016), the least support vector machine (Pham et al., 2018), and the Gini information gain (Quinlan, 1993). The Gini information gain method, using the RF approach (Liu et al., 2020; Zhang et al., 2020), was adopted in this study to assess the relative importance of each key factor. Information gain is used to determine which feature gives the maximum information for predicted results. It is based on the degree of uncertainty, impurity or disorder in the dataset. The Gini index is the probability of a randomly chosen feature being misclassified with a range between 0 and 1, where 0 denotes that all features belong to one class and 1 denotes that the features are randomly distributed across the class. The Gini index is calculated by

$$\text{Gini} = 1 - \sum_{i=1}^j p_i^2, \quad (4)$$

where  $p_i$  is the probability of a feature being classified into the class, and  $j$  is the number of features in the class.

Table 2 presents the importance of the selected key factors (precipitation, dam reservoir level, and landslide evolution state) on the prediction of periodic displacement. An evaluation and comparison of the predictive capability of the key influencing factors using the Gini information gain method indicate that the significance of the precipitation, dam reservoir level, and landslide evolution state varies from one

Table 2 Inputs for periodic displacement modelling and their importance

Input		Importance of influencing factor		
		Baishuihe landslide	Bazimen landslide	Baijiabao landslide
Precipitation	Input 1, the 1-month cumulative antecedent rainfall	0.03	0.12	0.04
	Input 2, the 2-month cumulative antecedent rainfall	0.03	0.07	0.04
Dam reservoir level	Input 3, reservoir level change in 1-month period	0.04	0.21	0.23
	Input 4, reservoir level change in 2-month period	0.07	–	–
	Input 5, the average elevation of the dam reservoir level in the current month	0.04	–	0.04
Landslide evolution state	Input 6, the displacement over the past 1 month	0.05	0.06	0.02
	Input 7, the displacement over the past 2 months	0.07	0.07	0.03
	Input 8, the displacement over the past 3 months	0.66	0.47	0.60

landslide to the other for different selected inputs. The results of the Gini information gain analysis show that the displacement (called landslide evolution state in Table 2) over the past three months has the highest significance for the three landslides. The respective influence factors can be explained as follows:

1. Machine learning algorithms were used to predict the periodic displacement in the forthcoming month from the displacement over earlier periods of either one, two, or three months. The predicted displacements were more dependent on the earlier displacements than those on the seasonal rainfall.

2. Precipitation showed a lower significance index than the dam reservoir water level for the three landslides. Most of the landslide bodies were submerged in the reservoir water. The portion of the landslide affected by rainfall was therefore limited.

### 5.3 Prediction process with the machine learning and polynomial models

Fig. 7 describes the prediction process with machine learning and polynomial models, including model training and testing. The trend and dynamic components of the accumulated landslide displacement were predicted separately. The trend displacement was constructed by fitting a curve to the trend displacement. The periodic displacement was predicted by the machine learning models. The total accumulated displacement was obtained by adding the predicted trend and periodic displacements. The predicted total displacement was then compared with the monitoring data. Once the model was established (using 70% of the monitoring data), the model was

then tested, following the same process with the remaining 30% of the data.

## 6 Results

### 6.1 Displacement decomposition

Locations with detailed displacement measurements were selected for detailed analysis to develop the machine learning model and to test the landslide displacement prediction model. Locations included Location ZG118 for the Baishuihe landslide, Location ZG111 for the Bazimen landslide, and Location ZG324 for the Baijiabao landslide.

1. At Location ZG118 on the Baishuihe landslide, the first 113 readings of monitoring data, from August 2003 to December 2012, were used to train (i.e. learn) the machine learning models. The remaining 12 readings, collected from January to December 2013, were used to verify the prediction reliability of the model.

2. At Location ZG111 on the Bazimen landslide, the monitoring data from August 2003 to December 2011 were used to train the model and the remaining data from January 2012 to December 2012 were used to validate the model.

3. At Location ZG324 on the Baijiabao landslide, the monitoring data from January 2007 to December 2012 were used as training dataset while the data from January 2013 to December 2013 were used to test the model.

For the three landslides, the decomposition of the displacement was calculated using the moving average method using 12 months as the cycle interval. The measured periodic term, after removal of the trend term from the total displacement, was modelled with each of the three machine learning algorithms. Fig. 8 shows the trend term displacement and periodic term displacement as measured at Locations ZG118, ZG111, and ZG324 for each of the three landslides.

### 6.2 Prediction of trend displacement

The trend displacement component was modelled with a cubic polynomial function (Eq. (2)). For Locations ZG118 and ZG324, the trend displacement was divided into three segments. The trend curve at Location ZG111 was divided into two segments.

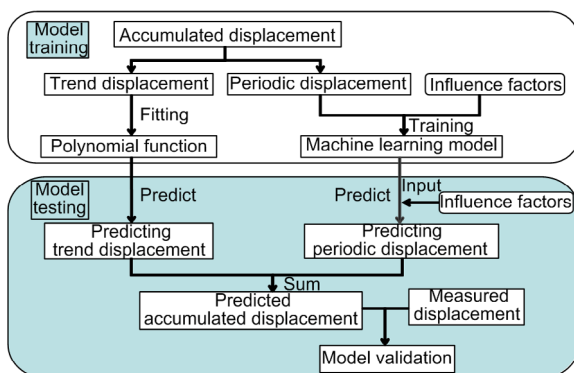
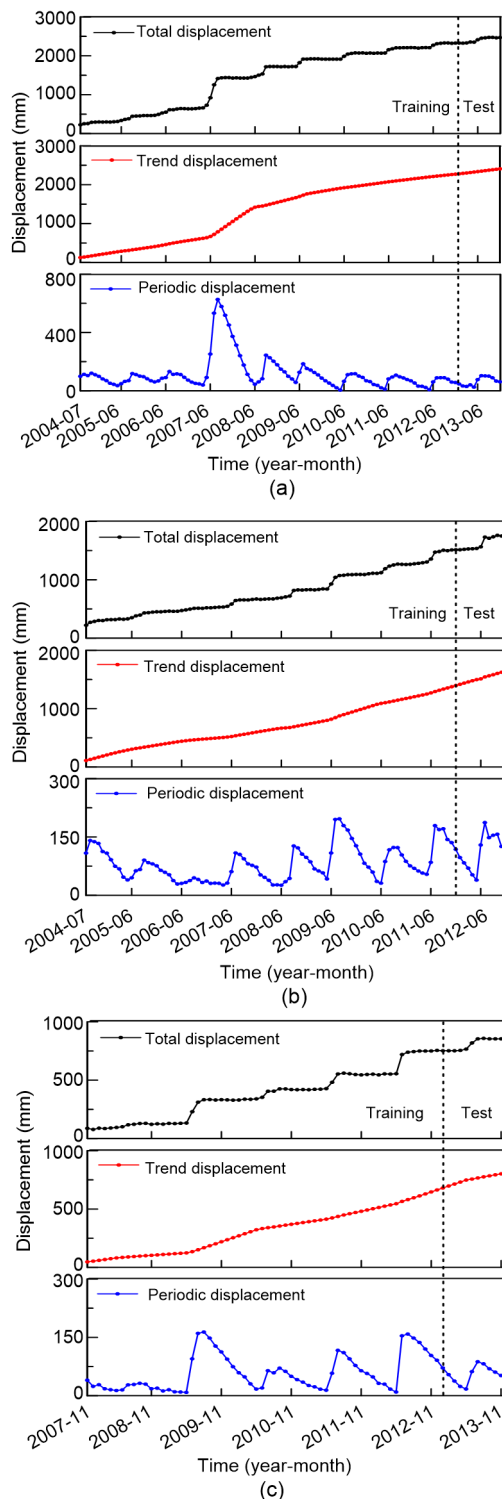


Fig. 7 Flowchart of the prediction model



**Fig. 8** Displacement decomposition into trend and periodic components at Locations ZG118, ZG111, and ZG324 (a) Baishuihe landslide (ZG118); (b) Bazimen landslide (ZG111); (c) Baijiabao landslide (ZG324)

Table 3 shows the cubic polynomial function for the training dataset for each landslide. The predicted trend displacement was calculated by the cubic polynomial function of the last training period. The predicted trend displacement calculated by the cubic polynomial function agrees well with the measured data, as illustrated in Fig. 9 and confirmed by the high regression coefficients  $R^2$  in Table 3.

### 6.3 Prediction of periodic displacement

The dataset was divided into a training and a validation set. Xu and Niu (2018) suggested dividing the data population into two parts with 70% for training and 30% for validation. Using this approach, they developed a well-trained LSTM model. This division of 70/30 was selected for the present study. In each location, where a prediction was undertaken, the periodic term displacements and controlling factors were normalized to  $[-1, 1]$ .

The grid search method was used to search for the optimal parameters of the three machine learning models. With the LSTM algorithm, the models for the Baishuihe, Bazimen, and Baijiabao landslides had three hidden layers. With the GRU algorithm, the models at Baishuihe and Bazimen landslides had three hidden layers while Baijiabao landslide model had only two hidden layers. The optimal length of the input sequence for the LSTM and GRU was also determined by the grid search method and was finally set to 12. RF is an ensemble algorithm based on decision trees. The numbers of decision trees for the Baishuihe, Bazimen, and Baijiabao RF models were 75, 100, and 10, respectively. The displacement prediction results of the analyses with the three machine learning algorithms were: (1) the displacements calculated for the training dataset and for the validation dataset over the entire observation period for the LSTM, RF, and GRU models are compared with the measured displacements; (2) the detailed predicted displacements for the three landslides are calculated by three algorithms over the validation dataset; (3) the accuracy of the three machine learning models is compared.

Fig. 10 compares the measured and predicted periodic displacements during the training process at Locations ZG118, ZG111, and ZG324 using the LSTM, GRU, and RF models. During the training, the

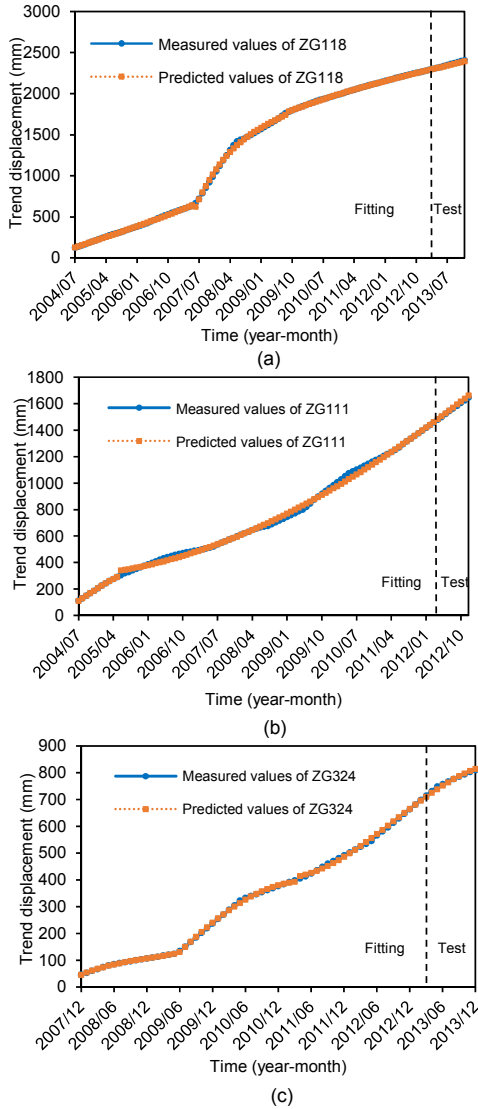


**Fig. 9 Predicted and measured trend displacement components**  
 (a) Baishuihe landslide; (b) Bazimen landslide; (c) Baijiabao landslide

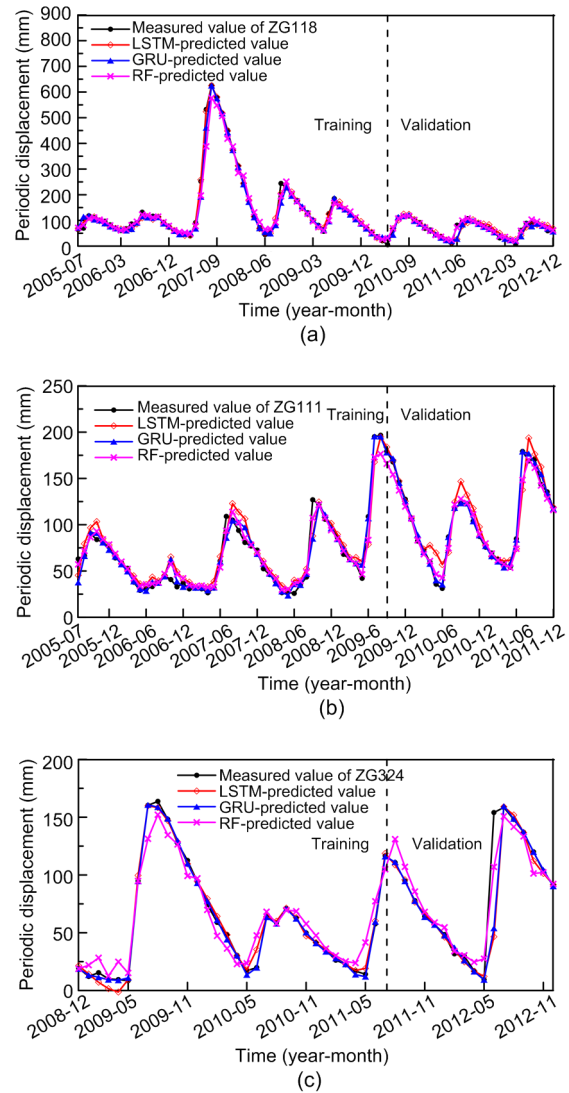


**Fig. 10 Comparison of measured and predicted displacements for training and validation datasets, using the LSTM, GRU, and RF machine learning models**  
 (a) Baishuihe landslide; (b) Bazimen landslide; (c) Baijiabao landslide

**Table 3 Coefficients of trend displacement polynomial function ( $\phi(t)=at^3+bt^2+ct+d$ )**

Landslide	Time period	<i>a</i>	<i>b</i>	<i>c</i>	<i>d</i>	Regression coefficient ( <i>R</i> <sup>2</sup> )
Baishuihe ZG118	July 2004–May 2007	0.0010	−0.0065	14.055	114.74	0.999
	June 2007–Aug. 2009	0.0441	−3.9100	98.947	529.50	0.996
	Sept. 2009–Dec. 2012	0.0009	−0.1303	16.382	1766.30	1.000
Bazimen ZG111	July 2004–May 2005	−0.0378	0.4454	17.569	93.32	1.000
	June 2005–Dec. 2011	−0.0002	−0.1269	4.6793	335.22	0.997
Baijiabao ZG324	Dec. 2007–May 2009	0.0113	−0.4603	9.4709	37.10	0.999
	June 2009–Feb. 2011	−0.0067	−0.1816	20.059	110.90	0.998
	Mar. 2011–Dec. 2012	−0.0125	0.6852	3.2434	410.56	0.995

computed displacements agreed well with the measured displacements for the three machine learning algorithms. Based on these results, the established LSTM, GRU, and RF models were judged to be adequate to predict the periodic displacement under future conditions.

Fig. 11 compares the measured and predicted displacements for the three landslides with the three machine learning algorithms in more detail, but this time using the testing dataset only. The periodic landslide displacement was initiated and aggravated by rainfall and dam reservoir water level which change periodically every year in the Three Gorges

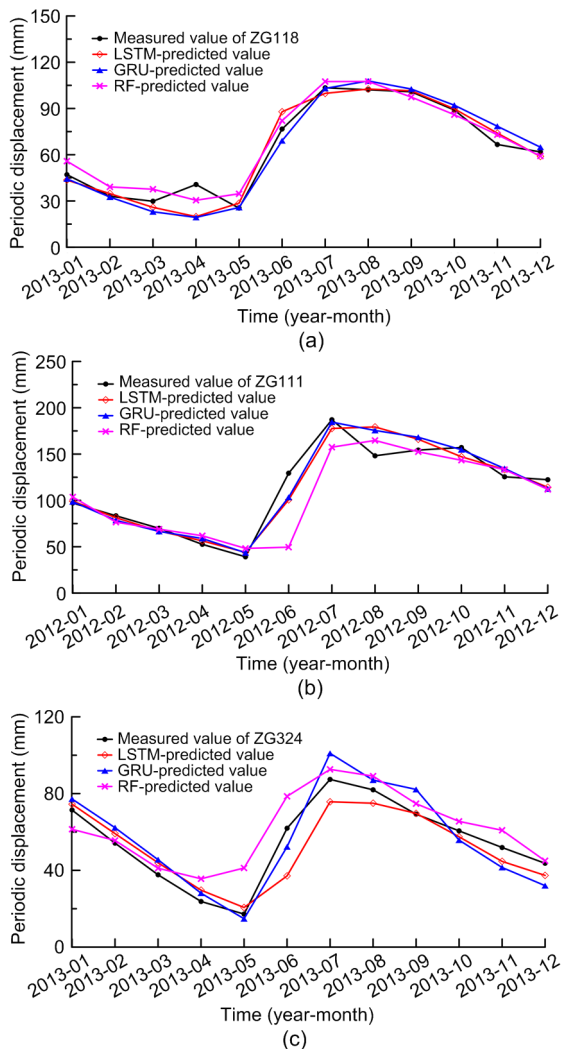


**Fig. 11 Comparison of measured and predicted periodic displacements for the validation dataset only, using the LSTM, GRU, and RF machine learning models**

(a) Baishuihe landslide; (b) Bazimen landslide; (c) Baijiabao landslide

reservoir area. For example, as shown in Fig. 4, the reservoir level was raised every October and held constant until April of the next year. The annual variation of rainfall was similar. Therefore, one year of testing dataset contained the seasonal variation of periodic displacement from these two external factors.

To quantify how well each of the machine learning models duplicates the measured displacements calculated under model testing, the following indicators were used: absolute error in mm, relative error in %, including their minimum and maximum values, the mean absolute percentage error (MAPE) in %, and the root mean square error (RMSE) in mm, defined as the standard deviation of the residuals. The RMSE tells how concentrated the data are around the line of best fit.

Tables 4–6 compare the measured and predicted periodic displacements with the testing dataset for the three landslides (Locations ZG118, ZG111, and ZG324), respectively with the LSTM, GRU, and RF machine learning models.

For the Baishuihe landslide (Location ZG118), the RMSE values with the LSTM, GRU, and RF models were very close, i.e. 7.5 mm, 8.0 mm, and 6.5 mm, respectively (Table 4). The range of absolute errors from the RF model is the smallest, with a minimum error of 2.7 mm and a maximum error of 10.2 mm. The MAPE values were 10.5%, 10.7%, and 13.5% for the LSTM, GRU, and RF models, respectively.

For the Bazimen landslide (Location ZG111), the RMSE values with the LSTM, GRU, and RF models were 13.8 mm, 12.6 mm, and 26.0 mm, respectively (Table 5). The MAPE values were 8.6%, 8.4%, and 14.2% for the LSTM, GRU, and RF models, respectively.

For the Baijiabao landslide (Location ZG324), the RMSE values with the LSTM, GRU, and RF models were again very close, 9.2 mm, 8.8 mm, and 10.5 mm, respectively (Table 6, p.425). The MAPE values were 14.2%, 15.6%, and 24.4% for the LSTM, GRU, and RF models, respectively.

#### 6.4 Prediction of total accumulated displacement

The total displacement was obtained from the sum of the predicted trend and periodic displacements. Fig. 12 (p.425) shows the predicted total displacement calculated by cubic polynomial function and the LSTM, GRU, and RF machine learning

**Table 4 Comparison of accuracy of predicted periodic displacement at location ZG118 with three machine learning algorithms (Baishuihe landslide)**

Time (year-month)	Measured displ. (mm)	LSTM model			GRU model			RF model		
		Displ. (mm)	Absolute error (mm)	Relative error (%)	Displ. (mm)	Absolute error (mm)	Relative error (%)	Displ. (mm)	Absolute error (mm)	Relative error (%)
2013-01	47.1	43.6	3.5	7.5	44.4	2.7	5.7	55.8	8.8	18.6
2013-02	33.0	34.8	1.8	5.2	32.5	0.5	1.6	39.1	6.1	18.5
2013-03	29.8	25.9	3.9	13.3	23.0	6.8	22.9	37.6	7.8	26.2
2013-04	40.7	19.9	20.8	51.2	19.4	21.3	52.5	30.5	10.2	25.1
2013-05	25.4	28.6	3.2	12.9	25.8	0.4	1.7	34.7	9.3	36.8
2013-06	76.7	87.9	11.2	14.6	69.1	7.5	9.8	82.1	5.4	7.1
2013-07	103.4	99.8	3.6	3.5	103.0	0.4	0.4	107.5	4.0	3.9
2013-08	102.1	102.6	0.5	0.5	107.9	5.7	5.6	107.5	5.4	5.3
2013-09	100.8	101.5	0.7	0.7	102.6	1.8	1.8	97.4	3.5	3.4
2013-10	89.0	89.8	0.8	0.9	92.1	3.1	3.5	86.0	3.0	3.4
2013-11	66.6	74.0	7.4	11.0	78.5	11.8	17.8	73.0	6.4	9.5
2013-12	61.8	58.9	2.9	4.7	64.9	3.1	5.0	59.2	2.7	4.3
Min. error	–	–	0.5	0.5	–	0.4	0.4	–	2.7	3.4
Max. error	–	–	20.8	51.2	–	21.3	52.5	–	10.2	36.8
MAPE (%)	–	–	5.0	10.5	–	5.4	10.7	–	6.0	13.5
RMSE (mm)	–	7.5	–	–	8.0	–	–	6.5	–	–

**Table 5 Comparison of accuracy of predicted periodic displacement at location ZG111 with three machine learning algorithms (Bazimen landslide)**

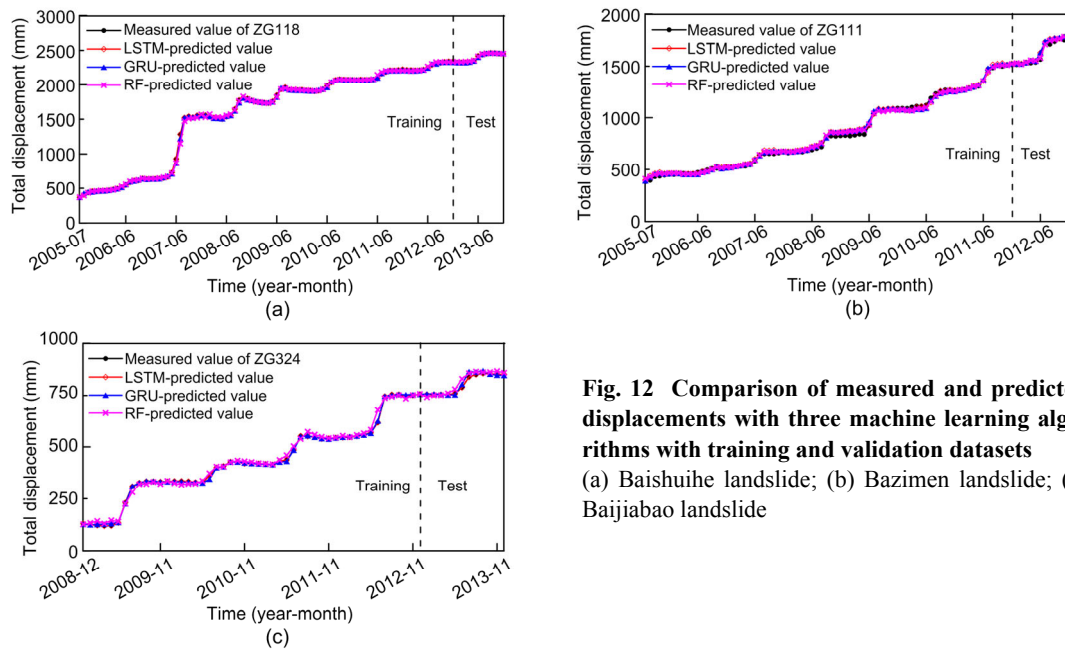
Time (year-month)	Measured displ. (mm)	LSTM model			GRU model			RF model		
		Displ. (mm)	Absolute error (mm)	Relative error (%)	Displ. (mm)	Absolute error (mm)	Relative error (%)	Displ. (mm)	Absolute error (mm)	Relative error (%)
2012-01	97.2	99.2	2.0	2.1	98.6	1.4	1.5	103.7	6.5	6.7
2012-02	83.4	81.3	2.1	2.5	78.5	4.9	5.9	76.5	6.9	8.3
2012-03	69.9	67.0	2.9	4.2	66.5	3.3	4.8	69.0	0.9	1.3
2012-04	52.6	56.4	3.8	7.1	58.9	6.3	12.0	61.9	9.3	17.6
2012-05	39.1	43.9	4.8	12.3	43.5	4.4	11.2	48.2	9.1	23.1
2012-06	129.4	100.7	28.7	22.2	103.4	26.0	20.1	49.5	79.8	61.7
2012-07	187.1	177.7	9.4	5.0	184.5	2.6	1.4	157.5	29.6	15.8
2012-08	148.2	179.3	31.1	21.0	175.5	27.3	18.4	164.7	16.6	11.2
2012-09	154.3	166.0	11.7	7.6	168.2	13.9	9.0	152.5	1.9	1.2
2012-10	157.1	147.2	10.0	6.3	154.7	2.4	1.5	143.3	13.8	8.8
2012-11	125.5	133.3	7.8	6.2	134.4	8.9	7.1	133.3	7.7	6.2
2012-12	122.3	114.2	8.2	6.7	112.4	9.9	8.1	111.9	10.4	8.5
Min. error	–	–	2.0	2.1	–	1.4	1.4	–	0.9	1.2
Max. error	–	–	31.1	22.2	–	27.3	20.1	–	79.8	61.7
MAPE (%)	–	–	10.2	8.6	–	9.3	8.4	–	16.0	14.2
RMSE (mm)	–	13.8	–	–	12.6	–	–	26.0	–	–

models. The results indicate that the prediction of three models agrees well with the measurements. Between January and December 2013 for the Baishuihe landslide (Location ZG118), the RMSE values in the predicted total displacement were 10.9 mm, 10.0 mm, and 10.1 mm, respectively with the LSTM, GRU, and RF models. For the Bazimen landslide (Location ZG111),

the RMSE values in the predicted total displacement were 20.0 mm, 19.5 mm, and 26.9 mm between January and December 2012, respectively with the LSTM, GRU, and RF models. For the Baijiabao landslide (Location ZG324), the RMSE values over 2013 were 10.2 mm, 8.9 mm, and 8.4 mm with the LSTM, GRU, and RF models, respectively.

**Table 6 Comparison of accuracy of predicted periodic displacement at location ZG324 with three machine learning algorithms (Baijiabao landslide)**

Time (year-month)	Measured displ. (mm)	LSTM model			GRU model			RF model		
		Displ. (mm)	Absolute error (mm)	Relative error (%)	Displ. (mm)	Absolute error (mm)	Relative error (%)	Displ. (mm)	Absolute error (mm)	Relative error (%)
2013-1	71.4	74.5	3.1	4.3	77.2	5.8	8.1	61.4	10.0	14.0
2013-2	54.2	59.2	5.0	9.2	62.2	8.0	14.8	55.6	1.4	2.6
2013-3	37.7	44.0	6.3	16.6	45.5	7.9	20.9	41.1	3.4	9.1
2013-4	23.8	29.7	5.9	24.8	28.1	4.3	18.2	35.6	11.8	49.8
2013-5	17.2	20.6	3.4	19.9	14.8	2.4	14.1	41.2	24.0	139.5
2013-6	61.9	37.1	24.8	40.1	52.3	9.6	15.6	78.6	16.7	26.9
2013-7	87.4	75.7	11.7	13.4	101.0	13.6	15.5	92.6	5.2	6.0
2013-8	82.0	75.0	7.0	8.5	87.0	5.1	6.2	89.1	7.2	8.7
2013-9	69.3	69.7	0.4	0.6	82.2	12.9	18.6	74.7	5.5	7.9
2013-10	60.6	57.5	3.1	5.1	55.7	4.8	8.0	65.5	4.9	8.2
2013-11	51.9	44.7	7.2	14.0	41.5	10.4	20.1	60.9	9.0	17.3
2013-12	43.7	37.4	6.3	14.4	32.0	11.7	26.7	45.0	1.3	3.0
Min. error	–	–	0.4	0.6	–	2.4	6.2	–	1.3	2.6
Max. error	–	–	24.8	40.1	–	13.6	26.7	–	24.0	139.5
MAPE (%)	–	–	7.0	14.2	–	8.0	15.6	–	8.4	24.4
RMSE (mm)	–	9.2	–	–	8.8	–	–	10.5	–	–

**Fig. 12 Comparison of measured and predicted displacements with three machine learning algorithms with training and validation datasets (a) Baishuihe landslide; (b) Bazimen landslide; (c) Baijiabao landslide**

## 7 Discussion

Current traditional machine learning algorithms predict landslide displacement as static regressions. However, landslide processes are nonlinear, dynamic phenomena that occur over time suggesting that dynamic modelling is more suitable for predicting

displacements caused by landslides. In this study, dynamic models used time series analysis to predict landslide displacements. Two algorithms, LSTM and GRU, were neural network algorithms.

The three machine learning models used in this paper, the LSTM, GRU, and RF algorithms, were able to predict with reasonable accuracy of the periodic

and total accumulated displacement of three step-wise landslides in the Three Gorges Dam reservoir area. The models established relationships among the data at different times, the state of the landslide displacements and the rainfall, and water level draw-down (and rise) in the dam reservoir. The algorithms were able to learn rules from earlier time steps and historical information.

Table 7 compares the accuracy indicators MAPE and RMSE for the three machine learning models for each of the three landslides. The predictions by the LSTM and GRU models were similar and had approximately the same margin of error. For the Baishuihe and Baijiabao landslides, the results with the three machine learning algorithms were approximately equivalent. The RMSE values are less than 10 mm and the MAPE values are between 10% and 16% for the LSTM and the GRU models. The LSTM neural network and the GRU models agreed especially well with the measurements during the period of the step-wise increase in the displacement (May to July), as illustrated in Fig. 11. The RF model gives higher values of MAPE, although the RMSE values are similar to those from the other models. For the Bazimen landslide, the LSTM and GRU models appear to predict the displacement more reliably than the RF model. The reason for this difference might be because the RF algorithm, as a combination of binary decision trees, is not able to predict time-series observations as well as the other deep learning algorithms.

**Table 7 Comparison of accuracy of predicted periodic displacement for three landslides**

Landslide	MAPE (%)			RMSE (mm)		
	LSTM	GRU	RF	LSTM	GRU	RF
Baishuihe	10.5	10.7	13.5	7.5	8.0	6.5
Bazimen	8.6	8.4	14.2	13.8	12.6	26.0
Baijiabao	14.2	15.6	24.4	9.2	8.8	10.5

The proposed dynamic modeling approaches, using time-series analysis and machine learning models, resulted in accurate prediction of displacements for slow, step-wise deformations. For the three landslides, rainfall and the reservoir water level fluctuation were the key external factors leading to increased slope displacements. The respective im-

portance of each of the rainfall and reservoir water level was not, however, the same over time. The displacement response, depending on the respective influence factors may result in a change in the learned rules during the training of the model. The LSTM and GRU machine learning models were able to adapt to these changes, through assessing the learned rules, forgetting invalid ones and remembering useful ones.

Since the multivariate LSTM and GRU algorithms provide an accurate prediction of the step-wise displacements in the Three Gorges Dam reservoir, such models could be very useful in early warning systems. Based on this study, the LSTM and GRU models can be recommended to predict landslide displacement in the Three Gorges Dam reservoir area. Note that fewer hyper-parameters need to be tuned in the GRU model than those in the LSTM model. The RF model needs more validation, in view of the results obtained in this study.

There are two main limitations to the analyses done: (1) at this time, the good agreement obtained applies to step-wise type of landslide movements only; (2) for each landslide studied, one monitoring point was used: a single point is insufficient to characterize an entire landslide. The analysis should be expanded to include several monitoring points in different parts of each landslide. This would also increase the quantity of data for the machine learning models, which would be beneficial. This would lead to an improved estimation of the predictive capability of the three different models.

## 8 Conclusions

The goal of this research was to test and compare different machine learning algorithms in predicting landslide displacements in the Three Gorges Dam reservoir area to see if such displacements predicted by machine learning models can be used as an input in landslide early warning systems. The paper also aims at demonstrating the maturity of machine learning algorithms and their use in geotechnical engineering models.

The three machine learning models (LSTM, GRU, and RF) were able to accurately predict periodic and total accumulated displacement for the three step-wise landslides in the Three Gorges Dam

reservoir area. The models established relationships among the data at different times, the state of the landslide displacements, and the causal effects of rainfall and water level drawdown (and rise) in the dam reservoir. The LSTM and GRU algorithms were able to learn rules from earlier time steps, thus making use of the historical information.

The proposed dynamic modelling approach, using time series analysis and machine learning models, also had accurate results in predicting displacements for slow and step-wise deformations. The LSTM and GRU machine learning models were able to adapt to these changes, through assessing the learned rules, forgetting invalid ones, and remembering useful ones.

The results of the analysis indicate that predictive models should become an essential component in landslide early warning systems. Multivariate LSTM and GRU machine learning algorithms could be very useful as one of the “risk-informed” inputs in an early warning system to help decision-making. Overall, dynamic models based on machine learning outputs have the potential for broad applications to predict landslide displacement in landslide-prone regions and should be further studied and refined to improve their accuracy.

### Contributors

The overarching research goals were developed by Suzanne LACASSE, Zhong-qiang LIU, and Jin-hui LI. Zhong-qiang LIU and Bei-bei YANG provided the measured landslides displacement data, and analyzed the measured data. Jin-hui LI, Dong GUO, and Bei-bei YANG established the models and calculated the predicted displacement. Zhong-qiang LIU and Jin-hui LI analyzed the calculated results. The initial draft of the manuscript was written by Zhong-qiang LIU, Jung-chan CHOI, and Dong GUO. All authors replied to reviewers' comments and revised the final version.

### Conflict of interest

Zhong-qiang LIU, Dong GUO, Suzanne LACASSE, Jin-hui LI, Bei-bei YANG, and Jung-chan CHOI declare that they have no conflict of interest.

### References

Bai SB, Wang J, Lü GN, et al., 2010. GIS-based logistic regression for landslide susceptibility mapping of the Zhongxian segment in the Three Gorges area, China. *Geomorphology*, 115(1-2):23-31.  
<https://doi.org/10.1016/j.geomorph.2009.09.025>

Breiman L, 2001. Random forests. *Machine Learning*, 45(1): 5-32.  
<https://doi.org/10.1023/A:1010933404324>

Cao Y, Yin KL, Alexander DE, et al., 2016. Using an extreme learning machine to predict the displacement of step-like landslides in relation to controlling factors. *Landslides*, 13(4):725-736.  
<https://doi.org/10.1007/s10346-015-0596-z>

Chen SY, Chou WY, 2012. Short-term traffic flow prediction using EMD-based recurrent hermite neural network approach. Proceedings of the 15th International IEEE Conference on Intelligent Transportation Systems, p.1821-1826.  
<https://doi.org/10.1109/ITSC.2012.6338665>

CIGM (China Institute of Geo-environment Monitoring), 2017. Bulletin of geologic hazards from January to December in 2016. China Institute of Geo-environment Monitoring, Beijing, China (in Chinese).

Cho K, van Merriënboer B, Gulcehre C, et al., 2014. Learning phrase representations using RNN encoder-decoder for statistical machine translation. Proceedings of the Conference on Empirical Methods in Natural Language Processing, p.1724-1734.

Corominas J, Moya J, Ledesma A, et al., 2005. Prediction of ground displacements and velocities from groundwater level changes at the Vallcebre landslide (Eastern Pyrenees, Spain). *Landslides*, 2(2):83-96.  
<https://doi.org/10.1007/s10346-005-0049-1>

Crozier MJ, Glade T, 2005. Landslide hazard and risk: issues, concepts and approach. In: Glade T, Anderson M, Crozier MJ (Eds.), *Landslide Hazard and Risk*. John Wiley and Sons Ltd., p.1-40.  
<https://doi.org/10.1002/9780470012659.ch1>

Du J, Yin KL, Lacasse S, 2013. Displacement prediction in colluvial landslides, Three Gorges reservoir, China. *Landslides*, 10(2):203-218.  
<https://doi.org/10.1007/s10346-012-0326-8>

Han M, Xi JH, Xu SG, et al., 2004. Prediction of chaotic time series based on the recurrent predictor neural network. *IEEE Transactions on Signal Processing*, 52(12):3409-3416.  
<https://doi.org/10.1109/TSP.2004.837418>

Huang FM, Yin KL, Zhang GR, et al., 2016. Landslide displacement prediction using discrete wavelet transform and extreme learning machine based on chaos theory. *Environmental Earth Sciences*, 75(20):1376.  
<https://doi.org/10.1007/s12665-016-6133-0>

Intrieri E, Raspini F, Fumagalli E, et al., 2018. The Maoxian landslide as seen from space: detecting precursors of failure with Sentinel-1 data. *Landslides*, 15:123-133.  
<https://doi.org/10.1007/s10346-017-0915-7>

Li JH, Li PX, Guo D, et al., 2020. Advanced prediction of tunnel boring machine performance based on big data. *Geoscience Frontiers*, in press.  
<https://doi.org/10.1016/j.gsf.2020.02.011>

- Liu ZB, Shao JF, Xu WY, et al., 2014. Comparison on landslide nonlinear displacement analysis and prediction with computational intelligence approaches. *Landslides*, 11(5):889-896.  
<https://doi.org/10.1007/s10346-013-0443-z>
- Liu ZQ, Gilbert G, Cepeda JM, et al., 2020. Modelling of shallow landslides with machine learning algorithms. *Geoscience Frontiers*, in press.  
<https://doi.org/10.1016/j.gsf.2020.04.014>
- Ma JW, Tang HM, Liu X, et al., 2017. Establishment of a deformation forecasting model for a step-like landslide based on decision tree C5.0 and two-step cluster algorithms: a case study in the Three Gorges Reservoir area, China. *Landslides*, 14(3):1275-1281.  
<https://doi.org/10.1007/s10346-017-0804-0>
- Ma JW, Tang HM, Liu X, et al., 2018. Probabilistic forecasting of landslide displacement accounting for epistemic uncertainty: a case study in the Three Gorges Reservoir area, China. *Landslides*, 15(6):1145-1153.  
<https://doi.org/10.1007/s10346-017-0941-5>
- McDougall S, 2017. 2014 Canadian geotechnical colloquium: landslide runout analysis—current practice and challenges. *Canadian Geotechnical Journal*, 54(5):605-620.  
<https://doi.org/10.1139/cgj-2016-0104>
- Miao FS, Wu YP, Xie YH, et al., 2018. Prediction of landslide displacement with step-like behavior based on multialgorithm optimization and a support vector regression model. *Landslides*, 15(3):475-488.  
<https://doi.org/10.1007/s10346-017-0883-y>
- Pham BT, Prakash I, Tien Bui D, 2018. Spatial prediction of landslides using a hybrid machine learning approach based on Random Subspace and Classification and Regression Trees. *Geomorphology*, 303:256-270.  
<https://doi.org/10.1016/j.geomorph.2017.12.008>
- Qin SQ, Jiao JJ, Wang SJ, 2002. A nonlinear dynamical model of landslide evolution. *Geomorphology*, 43(1-2):77-85.  
[https://doi.org/10.1016/S0169-555X\(01\)00122-2](https://doi.org/10.1016/S0169-555X(01)00122-2)
- Quinlan JR, 1993. C4.5 Programs for Machine Learning. Morgan Kaufmann Publishers, California, USA, p.17-45.
- Ran QH, Su DY, Qian Q, et al., 2012. Physically-based approach to analyze rainfall-triggered landslide using hydraulic gradient as slide direction. *Journal of Zhejiang University-SCIENCE A (Applied Physics & Engineering)*, 13(12):943-957.  
<https://doi.org/10.1631/jzus.A1200054>
- Selby MJ, 1988. Landslides: causes, consequences and environment. *Journal of the Royal Society of New Zealand*, 18(3):343.  
<https://doi.org/10.1080/03036758.1988.10429158>
- Tien Bui D, Tuan TA, Klempe H, et al., 2016. Spatial prediction models for shallow landslide hazards: a comparative assessment of the efficacy of support vector machines, artificial neural networks, kernel logistic regression, and logistic model tree. *Landslides*, 13:361-378.  
<https://doi.org/10.1007/s10346-015-0557-6>
- Vincent P, Laroche H, Lajoie I, et al., 2010. Stacked denoising autoencoders: learning useful representations in a deep network with a local denoising criterion. *The Journal of Machine Learning Research*, 11(12):3371-3408.
- Xu SL, Niu RQ, 2018. Displacement prediction of Baijiabao landslide based on empirical mode decomposition and long short-term memory neural network in Three Gorges area, China. *Computers & Geosciences*, 111:87-96.  
<https://doi.org/10.1016/j.cageo.2017.10.013>
- Yang BB, Yin KL, Xiao T, et al., 2017. Annual variation of landslide stability under the effect of water level fluctuation and rainfall in the Three Gorges Reservoir, China. *Environmental Earth Sciences*, 76(16):564.  
<https://doi.org/10.1007/s12665-017-6898-9>
- Yang BB, Lacasse S, Yin KL, et al., 2018. Factors influencing landslide deformation from observations in the Three Gorges Reservoir. In: Wu W, Yu HS (Eds.), Proceedings of China-Europe Conference on Geotechnical Engineering. Springer, Switzerland, p.1551-1555.  
[https://doi.org/10.1007/978-3-319-97115-5\\_143](https://doi.org/10.1007/978-3-319-97115-5_143)
- Yang BB, Yin KL, Liu ZQ, et al., 2019a. Machine learning to predict landslide displacement in dam reservoir. Proceedings of the ICOLD Symposium, p.1-13.  
<https://doi.org/10.1201/9780429319778-270>
- Yang BB, Yin KL, Lacasse S, et al., 2019b. Time series analysis and long short-term memory neural network to predict landslide displacement. *Landslides*, 16(4):677-694.  
<https://doi.org/10.1007/s10346-018-01127-x>
- Zhang P, Yin ZY, Jin YF, et al., 2020. A novel hybrid surrogate intelligent model for creep index prediction based on particle swarm optimization and random forest. *Engineering Geology*, 265:105328.  
<https://doi.org/10.1016/j.enggeo.2019.105328>
- Zhou C, Yin KL, Cao Y, et al., 2016. Application of time series analysis and PSO-SVM model in predicting the Bazimen landslide in the Three Gorges Reservoir, China. *Engineering Geology*, 204:108-120.  
<https://doi.org/10.1016/j.enggeo.2016.02.009>
- Zhou C, Yin KL, Cao Y, et al., 2018a. Displacement prediction of step-like landslide by applying a novel kernel extreme learning machine method. *Landslides*, 15(11):2211-2225.  
<https://doi.org/10.1007/s10346-018-1022-0>
- Zhou C, Yin KL, Cao Y, et al., 2018b. Landslide susceptibility modeling applying machine learning methods: a case study from Longju in the Three Gorges Reservoir area, China. *Computers & Geosciences*, 112:23-27.

## 中文概要

题目：边坡位移智能预测算法

目的：边坡位移预测是实现滑坡灾害预报的有效手段，

对降低滑坡灾害造成的损失具有重要意义。本文针对三峡库区广泛分布的“阶跃型”滑坡，采用三种不同的机器学习算法：长短期记忆（LSTM）神经网络、随机森林（RF）算法和门控递归单元（GRU），预测三个不同的三峡库区边坡位移，并对比三种算法的预测精度，从而选择适用于边坡位移预测的机器学习算法。

**创新点：**1. 建立了基于时间序列分解和机器学习算法的动态预测模型，并能够准确预测边坡位移。2. 对比了不同的机器学习算法预测边坡周期项位移的精度。

**方法：**1. 基于时间序列分解原理，将边坡累积位移分解为趋势项位移和周期项位移。2. 利用多项式拟合对边坡趋势项位移进行预测。3. 基于位移影响因素采用三种机器学习模型（LSTM、GRU 和 RF）预测边坡周期项位移。

**结论：**1. 本文提出的基于时间序列分解和机器学习算法的动态预测模型可以准确预测三峡库区“阶跃型”边坡位移。2. LSTM 和 GRU 算法可以充分利用滑坡历史信息，精确预测边坡位移的周期项。

**关键词：**滑坡；位移；机器学习；三峡库区